JOURNAL OF VIROLOGY, June 2011, p. 6015–6023 Vol. 85, No. 12
0022-538X/11/$12.00 doi:10.1128/JVI.01537-10

Oncolytic Specificity of Newcastle Disease Virus Is Mediated by Selectivity for Apoptosis-Resistant Cells▽

Mena Mansour,[1,2] Peter Palese,[1,2] and Dmitriy Zamarin[1,2,3]*

Department of Medicine, Mount Sinai School of Medicine, New York, New York 10029[1]; Department of Microbiology, Mount Sinai School of Microbiology, New York, New York 10029[2]; and Department of Medicine, Memorial Sloan-Kettering Cancer Center, New York, New York 10065[3]

Received 22 July 2010/Accepted 29 March 2011

Newcastle disease virus (NDV) is a negative-sense RNA virus that has been shown to possess oncolytic activity. NDV's selective replication in tumor cells has been previously suggested to be due to the lack of a proper antiviral response in these cells. Here we demonstrate that NDV possesses oncolytic activity in tumor cells capable of a robust type I interferon (IFN) response, suggesting that another mechanism underlies NDV's tumor specificity. We show that the oncolytic selectivity of NDV for tumor cells is dependent upon tumor cell resistance to apoptosis. Utilizing the human non-small-cell lung cancer cell line A549 overexpressing the antiapoptotic protein Bcl-xL, we show significant enhancement of oncolytic activity and NDV replication. Interestingly, while the Bcl-xL-overexpressing cells were resistant to apoptotic stimuli induced by chemotherapeutic agents and early viral replication, during the subsequent viral cycles, we observed a paradoxical increase in apoptosis in response to NDV. The increased oncolytic activity seen was secondary to enhanced viral replication and syncytium formation. The induction of a type I IFN response was enhanced in Bcl-xL cells. Overall, these findings propose a new mechanism for cancer cell specificity for NDV, making it an attractive anticancer agent for chemoresistant tumors with enhanced antiapoptotic activity.

Newcastle disease virus (NDV) is a negative-sense single-stranded RNA virus of the *Paramyxoviridae* family that causes severe disease in several avian species (36). NDV has been shown to possess oncolytic properties (27, 32) and has been used as a cancer vaccine and also as an oncolytic agent in several clinical trials in different human cancers (14, 16, 21, 34). The selectivity of NDV and other oncolytic viruses to cancer cells has been proposed to be due to defects in the type I interferon (IFN) response of cancer cells (13, 38). These defects enhance the replication of NDV in cancer cells and hence increase their destruction.

Programmed cell death or apoptosis occurs naturally during development and aging and as a homeostatic mechanism for the survival of cell populations in tissues. Apoptosis is characterized by certain morphological and biochemical changes that are well described (9). The B-cell lymphoma 2 (Bcl-2) family of proteins is one of the most extensively studied regulators of apoptosis. Members of this family are either proapoptotic (Bax, Bak, and Bok) or antiapoptotic (Bcl-2, Bcl-xL, Bcl-W, and Mcl-10) or induce apoptosis by binding to antiapoptotic members of the family (Bid, Bim, Noxa, and PUMA) (46). Therapeutically, apoptosis is important, as many antineoplastic agents cause cellular damage by activating the apoptosis pathway. Resistance to these agents has been attributed to the overexpression of antiapoptotic proteins of the Bcl-2 family, especially Bcl-xL (22).

NDV has been shown to mediate its oncolytic effects through apoptosis induction in infected cells (19). Like many viruses, NDV induces apoptosis by activating the mitochondrial pathway (8, 31). This causes opening of mitochondrial permeability transition pores and loss of mitochondrial membrane potential, leading to release of SMAC/DIABLO and cytochrome *c*. SMAC/DIABLO causes suppression of inhibitory apoptosis proteins (IAP), while cytochrome *c* binds to apoptotic protease activator factor 1 (APAF-1) and procaspase 9, forming the apoptosome which activates apoptosis (9). This self-sacrifice of cells is an attempt to prevent further spread of the virus to neighboring cells. This defense may prove effective if cell death occurs before the assembly of more NDV progeny (36). It limits the spread of infection and hinders the oncolytic effects of NDV, especially if the virus is present at low concentrations.

Influenza virus NS1 protein is a strong antagonist of the type I IFN response and has been shown to possess antiapoptotic properties (51). In our previous studies, we demonstrated that NDV expressing influenza virus NS1 protein is an enhanced oncolytic agent that showed efficient replication in different cancer cells possessing a robust IFN response (44). NS1-expressing NDV, in addition, demonstrated enhanced syncytium formation in infected cancer cells. These findings were suggested to be due to the anti-IFN and possibly antiapoptotic effect of NS1 which helped prolong the survival of cancer cells and allowed the virus to replicate freely in the absence of an antiviral response. A similar mechanism was suggested in another recent study which showed enhanced oncolytic activity of NDV-HUJ in therapy-resistant melanoma specimens expressing the IAP Livin (20). These melanoma cells also have an intact IFN response. This raises questions about NDV's selectivity. Is the selective replication of NDV in cancer cells due in

* Corresponding author. Mailing address: Memorial Sloan-Kettering Cancer Center, Department of Medicine, 1275 York Avenue, Box #8, New York, NY 10065. Phone: (212) 639-5809. Fax: (212) 639-2283. E-mail: zamarind@mskcc.org.

▽ Published ahead of print on 6 April 2011.

part to defective apoptotic signaling in those cells? Can selective replication of NDV be independent of the IFN response?

In our current studies, we addressed these questions by utilizing human non-small-cell lung cancer (NSCLC) cell line A549 overexpressing the antiapoptotic protein Bcl-xL. We show that the oncolytic activity of NDV is significantly enhanced in apoptosis-resistant cells and is independent of the induction of a type I IFN response.

MATERIALS AND METHODS

Cell lines, antibodies, and reagents. A549-neo and A549–Bcl-xL cells were generated as described previously (48). 293-null and 293–Bcl-xL cells were purchased from Invivogen. A549-neo, A549–Bcl-xL, 293-null, 293–Bcl-xL, MDA-MB-468, MDA-MB-231, and Vero cells were maintained in Dulbecco's modified Eagle's medium (DMEM; Gibco) supplemented with 10% fetal bovine serum (JM Bioscience, San Diego, CA), penicillin, and streptomycin (Gibco). Monoclonal Bcl-xL antibody for Western blotting was from Pharmingen. NDV polyclonal rabbit serum was described previously (24, 49). β-Actin and tubulin monoclonal antibodies were from Sigma (St. Louis, MO). Alexa Fluor 488 dye-labeled anti-rabbit secondary antibody was from Molecular Probes (Eugene, OR). Z-VAD-FMK was from Sigma (St. Louis, MO).

Viruses. All of the viruses used in our studies were generated in our laboratory. NDV V (−)/NS1was generated by inserting a DNA fragment encoding the influenza virus A/PR8/34 NS1 protein between the HN and L genes as described previously (24). NDV V (−)/NS1, used in apoptosis studies, is in the NDV Hitchner B1 strain background and lacks expression of the V gene. For the rest of the studies, the NDV LaSota strain expressing green fluorescent protein (GFP) [NDV (LS)-GFP] was generated by inserting a DNA fragment encoding GFP between the P and M genes of NDV LaSota. NDV (LS)-GFP was used for easy detection of viral replication by GFP expression.

Caspase 3 assay. A549-neo and A549–Bcl-xL cells were infected with NDV (LS)-GFP at a multiplicity of infection (MOI) of 0.01 in 6-well plates. At specific time points, cells were washed with 1 ml phosphate-buffered saline (PBS) and collected by spinning at 1,500 rpm for 5 min at 4°C. The resulting pellet was flash-frozen and stored at −80°C until all samples were collected. Caspase 3 activity in the cells was measured using a Roche caspase 3 activity assay kit according to the instructions provided by the manufacturer. Caspase 3 activities in both cell lines are presented as absolute values. Results are from triplicate experiments.

Terminal deoxynucleotidyltransferase-mediated dUTP-biotin nick end labeling (TUNEL) staining and fluorescence-activated cell sorter (FACS) analysis. A549-neo and A549–Bcl-xL cells infected with NDV (LS)-GFP at an MOI of 0.01 were labeled using the APO-BrdU TUNEL assay kit (Invitrogen) according to the manufacturer's instructions. Briefly, cells were fixed using 1% paraformaldehyde for 15 min on ice and then permeabilized overnight using 70% ethanol. Cells were then stained for 1 h at 37°C with DNA labeling solution containing terminal deoxynucleotidyltransferase and bromodeoxyuridine (BrdU). Alexa Fluor 488 dye-labeled anti-BrdU antibody was used for secondary staining, and propidium iodide was used as a counterstain. Signals were then detected using an FC-500 flow cytometer from Beckman Coulter, and data were analyzed using FlowJo (Tree Star, Ashland, OR). Apoptosis was induced in both cell lines using staurosporine for positive controls, negative controls were noninfected cells, and a nonstained control was used to detect the baseline fluorescence in infected cells. All experiments were performed in triplicate.

LDH cytotoxicity assay. A549-neo cells, A549-neo cells pretreated with 20 nM Z-VAD-FMK, and A549–Bcl-xL cells were infected with NDV (LS)-GFP at an MOI of 0.01 in 6-well plates. At 24, 48, 72, and 96 h postinfection (hpi), cells were washed with 1 ml PBS and incubated with 1% Triton X for 20 min at 37°C. Lactate dehydrogenase (LDH) activity was measured using the Promega CytoTox 96 assay kit according to the instructions provided by the manufacturer. LDH assay results are presented as the ratio of infected to noninfected cell measurements. Results are from triplicate experiments.

Infections and virus titers. All cell lines were plated on 6-well plates at 24 h prior to infection. 293-null and 293–Bcl-xL cells were plated on poly-D-lysine-coated 6-well plates. On the day of infection, NDV (LS)-GFP was diluted to the required concentration in a solution of PBS, bovine serum albumin (BSA), calcium/magnesium, penicillin, and streptomycin. The virus was then added to the cells at the required MOI in a final volume of 200 μl, and the mixture was incubated for 1 h at room temperature. After 1 h, 2 ml of DMEM containing 0.3% BSA was added to the cells and the mixture was incubated at 37°C. The medium was supplemented with 1 μg/ml of tosylsulfonyl phenylalanyl chloromethyl ketone (TPCK) trypsin to activate NDV's fusion protein. Supernatants were collected at 24, 48, 72, and 96 hpi, and immunofluorescent labeling was used to determine virus titers in Vero cells.

Fluorescence microscopy. A549-neo and A549–Bcl-xL cells were cultured on 10-mm glass slides for 24 h prior to infection. Cells were then infected with NDV (LS)-GFP at an MOI of 0.01. After 20 h, cells were fixed using 5% formaldehyde and then permeabilized using 1% Triton X. Cells were then incubated with anti-NDV polyclonal serum for 2 h. An Alexa Fluor 488 dye-labeled anti-rabbit secondary antibody from Molecular Probes (Eugene, OR) was used to visualize NDV proteins. Nuclei were stained with 4′,6-diamidino-2-phenylindole (DAPI).

IFN induction bioassay. To detect IFN induction in A549-neo and A549–Bcl-xL cells, we used the bioassay previously described (25, 29). Briefly, A549-neo and A549–Bcl-xL cells were infected with NDV (LS)-GFP at an MOI of 0.01 and supernatants were collected every 3 h for 24 h. Viruses in the supernatant were UV inactivated by two pulses of 9,000 mJ/cm^2 using a Stratagene Stratalinker. Vero cells in 96-well plates were incubated overnight with the inactivated supernatants. Supernatants from uninfected cells and cells treated with 1,000 units of universal type I IFN (PBL, NJ) were used as negative and positive controls, respectively. Vero cells were then washed and subsequently infected with NDV (B1)-GFP at an MOI of 1. Eighteen hours later, GFP expression was visualized using an Olympus fluorescence microscope. Incubation of Vero cells with supernatants containing antiviral cytokines activates an antiviral state, causing inhibition of viral replication. Therefore, GFP expression is inversely proportional to the amount of IFN produced. Results were confirmed using quantitative real-time PCR (qRT-PCR) with human IFN-β (hIFN-β)-specific primers. For the IFN bioassay experiments with 293-null, 293–Bcl-xL, MDA-MB-231, and MDA-MB-468 cells, supernatants were collected at 24 h and serially diluted after UV inactivation. All bioassay experiments were performed in triplicate and repeated to confirm the results.

RNA extraction and qRT-PCR. qRT-PCR was performed as described before (12). Briefly, A549-neo and A549–Bcl-xL cells were infected with NDV (LS)-GFP at an MOI of 2. Cells were trypsinized, washed with PBS, and pelleted at the indicated time points. RNA was isolated and treated with DNase using the RNeasy minikit (Qiagen). RNA samples were quantified using a NanoDrop spectrophotometer (NanoDrop Technologies). RNA yields were approximately 50 to 100 μg per sample. qRT-PCR was performed using Brilliant II SYBR green (Stratagene) in a Bio-Rad CFX96 thermal cycler. Each transcript in each sample was assayed 3 times, and the mean cycle threshold was used to calculate the *n*-fold change and control changes for each gene. The 18S rRNA gene was used as a housekeeping gene. Data were analyzed as previously described (26).

siRNA design. Small interfering RNA (siRNA) targets were identified using the siRNA Selection Server (http://jura.wi.mit.edu/bioc/siRNAext/) (47). The targets used were CAGCUGGAGUCAGUUUAGU (siRNA 66), GAUGCAG GUAUUGGUGAGU (siRNA 473), and GGAACUCUAUGGGAACAAU (siRNA 575). Double-stranded siRNA was synthesized from DNA oligonucleotides using the *Silencer* siRNA construction kit (Ambion) according to the manufacturer's instructions. Cells were transfected with 5 nM Bcl-xL siRNA using Lipofectamine RNAiMax transfection reagent (Invitrogen). After 18 h, cells were infected with NDV (LS)-GFP at an MOI of 0.1. Supernatants were collected at 24, 48, and 72 hpi, and NDV titers were assessed. Results shown are from three independent experiments.

RESULTS

Expression of influenza virus NS1 protein by NDV delays apoptosis induction in infected cancer cells. NDV-NS1 is a recombinant NDV expressing influenza virus NS1 protein. We have previously demonstrated that NDV-NS1 possesses improved oncolytic activity both *in vitro* and *in vivo* and enhances syncytium formation, compared to that obtained with wild-type NDV (49). We hypothesized that the observed oncolytic enhancement could be in part due to antiapoptotic properties of NS1. To determine whether NS1 protein inhibits apoptosis in the context of NDV infection, we infected A549 cells with NDV-B1 and an NDV strain with a defective V protein expressing influenza virus NS1 protein [NDV V (−)/NS1] at an MOI of 0.01 and assessed the time course of apoptosis induction by caspase 3 activity assay (Fig. 1). Results showed lower

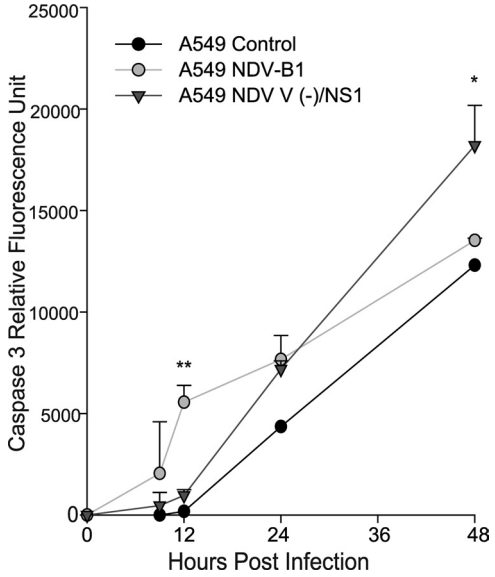

FIG. 1. NDV-NS1 delays apoptosis induction in A549 cells. A549 cells were infected with NDV V (−)/NS1 at an MOI of 0.01. NDV-B1 was used as a control. Cells were collected and flash-frozen, and caspase 3 activity was measured at 9, 12, 24, and 48 hpi. Caspase activity is presented as relative fluorescence units. *, $P < 0.05$; **, $P < 0.01$.

caspase 3 activity in cells infected with NDV V (−)/NS1 at earlier time points, which significantly increased at 48 h, consistent with the observed enhancement of cell death. We suspect that the early inhibition of apoptosis by NS1 may be responsible for the enhancement of the oncolytic activity of NDV due to increased viral replication and hypothesized that apoptosis resistance of cancer cells in general may be responsible for their susceptibility to NDV-mediated oncolysis.

A549–Bcl-xL cells are resistant to Bak overexpression and antineoplastic agents. To test our hypothesis, we utilized human NSCLC cell line A549 stably overexpressing the antiapoptotic protein Bcl-xL (A549–Bcl-xL). Overexpression is shown (Fig. 2A) by Western blotting for Bcl-xL in A549–Bcl-xL cells compared to control A549 cells expressing the gene encoding neomycin resistance (A549-neo). To demonstrate the resistance of A549–Bcl-xL cells to apoptosis, we transfected the cells with the gene for Bak or treated them with several antineoplastic agents (paclitaxel at 20 μM and etoposide at 150 μM) conventionally used in NSCLC treatment. As shown in Fig. 2B, overexpression of Bcl-xL dramatically reduced apoptosis induction in A549 cells by antineoplastic agents and Bak overexpression.

NDV induces efficient oncolysis in Bcl-xL-overexpressing cells. To compare the oncolytic effects of NDV in A549-neo and A549–Bcl-xL cells, we infected both cell lines with the NDV LaSota strain expressing GFP (LS-GFP) at an MOI of 0.01. Cytotoxicity was monitored at 24, 48, 72, and 96 hpi by LDH cytotoxicity assay (Fig. 3). As a control, A549-neo cells pretreated for 1 h with Z-VAD-FMK were also infected with LS-GFP. Interestingly, despite the resistance to apoptosis, we observed superior oncolytic activity in A549–Bcl-xL cells and A549-neo cells pretreated with Z-VAD-FMK compared to that in A549-neo cells.

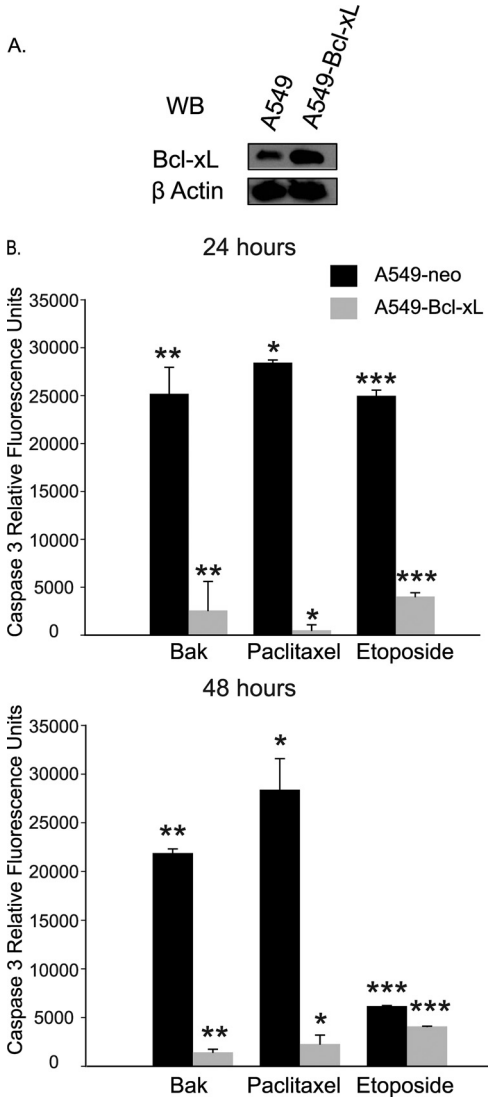

FIG. 2. A549 cells overexpressing Bcl-xL are resistant to apoptosis induction. (A) Bcl-xL overexpression in A549–Bcl-xL cells is shown by Western blotting (WB). (B) A549 and A549–Bcl-xL cells were either transfected with 500 ng of a Bak plasmid or treated with 20 μM paclitaxel or 150 μM etoposide, and caspase 3 activity was measured at 24 h (*, $P < 0.01$; **, $P < 0.005$; ***, $P < 0.004$) and 48 h (*, $P < 0.04$; **, $P < 0.016$; ***, $P < 0.015$).

NDV overcomes resistance to apoptosis in Bcl-xL-overexpressing cells. As the apoptosis-resistant cells were more susceptible to NDV oncolysis, we questioned whether this sensitivity parallels our findings with NDV V (−)/NS1, where early inhibition of apoptosis may be responsible for the enhanced viral replication, syncytium formation, and eventual cell killing seen. To compare apoptosis induction in A549-neo and A549–Bcl-xL cells, both cell lines were infected with NDV(LS)-GFP at an MOI of 0.01 and caspase 3 activity was measured at different time points postinfection (Fig. 4A). Similar to our findings with NDV V (−)/NS1, at early time points, caspase 3 activity was higher in A549-neo cells. Interestingly, at 36 hpi, A549–Bcl-xL cells show a dramatic increase in caspase 3 activity, with a peak at 48 hpi and then a decrease due to apop-

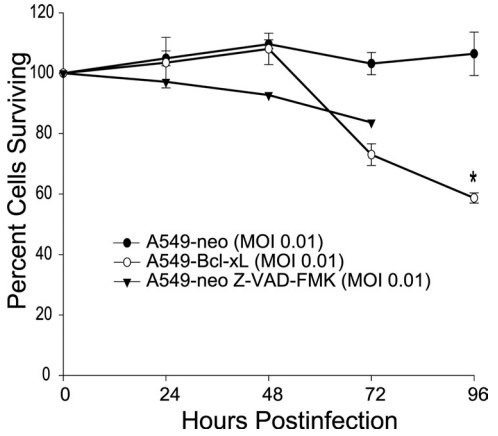

FIG. 3. NDV (LS)-GFP induces enhanced oncolysis in A549–Bcl-xL cells. A549-neo cells, A549-neo cells pretreated with Z-VAD-FMK, and A549–Bcl-xL cells were infected at an MOI of 0.01, and percentages of viable cells were determined by measuring LDH at 24, 48, 72, and 96 hpi. Values were normalized to noninfected A549 and A549–Bcl-xL cells ($P < 0.004$).

totic cell death. To determine whether the increased caspase 3 activity correlated with an increased number of cells undergoing apoptosis, we measured the percentage of apoptotic cells by TUNEL staining and flow cytometry analysis (Fig. 4B). There were significantly more A549–Bcl-xL than A549-neo cells undergoing apoptosis at 72 h, indicating that the increased number of apoptotic A549–Bcl-xL cells was responsible for the observed increase in caspase 3 activity. The observed delayed peak of apoptotic activity detected by TUNEL assay is likely a reflection of differences between the assays, with the TUNEL assay detecting later events in apoptosis induction (9).

The dramatic increase in caspase 3 activation and the number of apoptotic cells in the A549–Bcl-xL group were suggestive of a higher number of cells infected in the second and subsequent cycles of viral replication. In support of this, when a higher MOI was used, we observed an earlier peak of caspase 3 activation, but the relative levels of caspase 3 activity always remained higher in A549-neo than in A549–Bcl-xL cells (Fig. 4C). These data suggested that at a low MOI, inhibition of apoptosis in A549–Bcl-xL cells during the first cycle of replication may lead to the generation of higher viral titers, leading to a higher number of infected cells on the subsequent cycles and the observed increase in the number of apoptotic cells and caspase 3 activity.

Enhanced replication of NDV in Bcl-xL-overexpressing cells. To test this hypothesis, viral titers in A549-neo and A549–Bcl-xL cells were measured and compared (Fig. 5A). NDV (LS)-GFP showed significantly enhanced replication in A549–Bcl-xL cells, with a 2-log increase over that in A549-neo cells. This was coupled with enhanced syncytium formation by NDV (LS)-GFP in A549–Bcl-xL cells (Fig. 5B). Consistent with enhanced viral replication, as shown in Fig. 5C, NDV NP protein was detected at an earlier time point in A549–Bcl-xL than in A549-neo cells. These findings were confirmed in 293 cells overexpressing Bcl-xL (293–Bcl-xL), with a 2-log enhancement of NDV replication seen in 293–Bcl-xL cells compared to that of 293-null cells (Fig. 5D). To demonstrate that

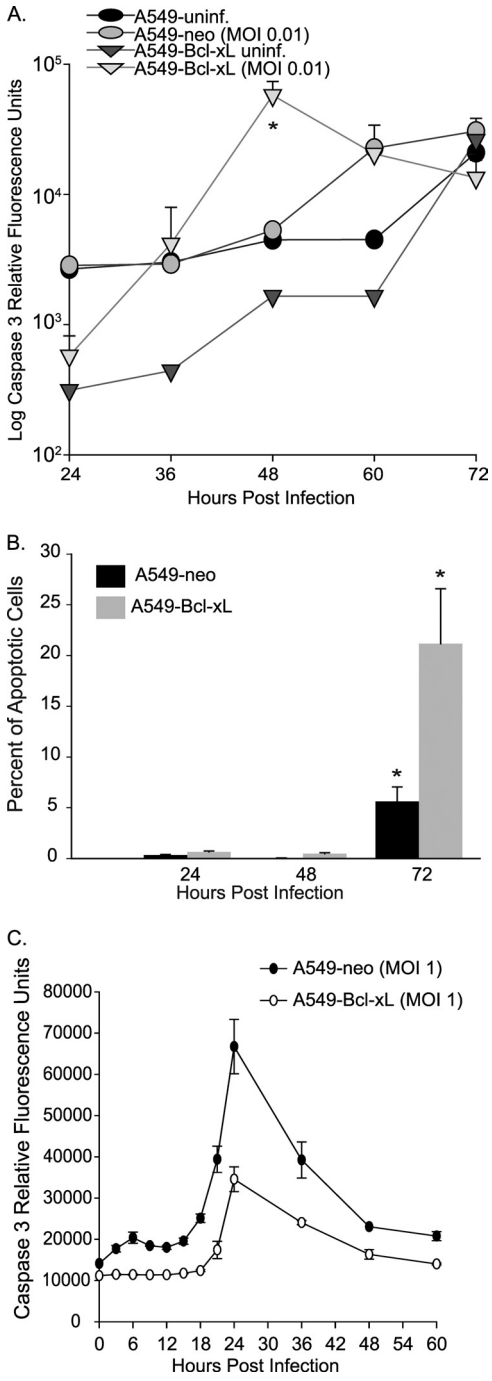

FIG. 4. NDV overcomes resistance to apoptosis in Bcl-xL-overexpressing cells. A549 and A549–Bcl-xL cells were infected at an MOI of 0.01. (A) Cells were collected and flash-frozen, and caspase 3 activity was measured at 24, 36, 48, 60, and 72 hpi. Caspase activity is presented as relative fluorescence units. *, $P < 0.03$. (B) TUNEL staining of infected cells analyzed by FACS showing percentages of apoptotic cells. *, $P < 0.05$. (C) Caspase 3 activity was measured in A549-neo and A549–Bcl-xL cells at different times postinfection at an MOI of 1.

the enhanced replication seen in A549–Bcl-xL cells is not due to enhanced cellular permissibility to initial NDV inoculation, both cell lines were infected with NDV (LS)-GFP at an MOI of 0.01. At the end of first replication cycle (18 hpi), cells were

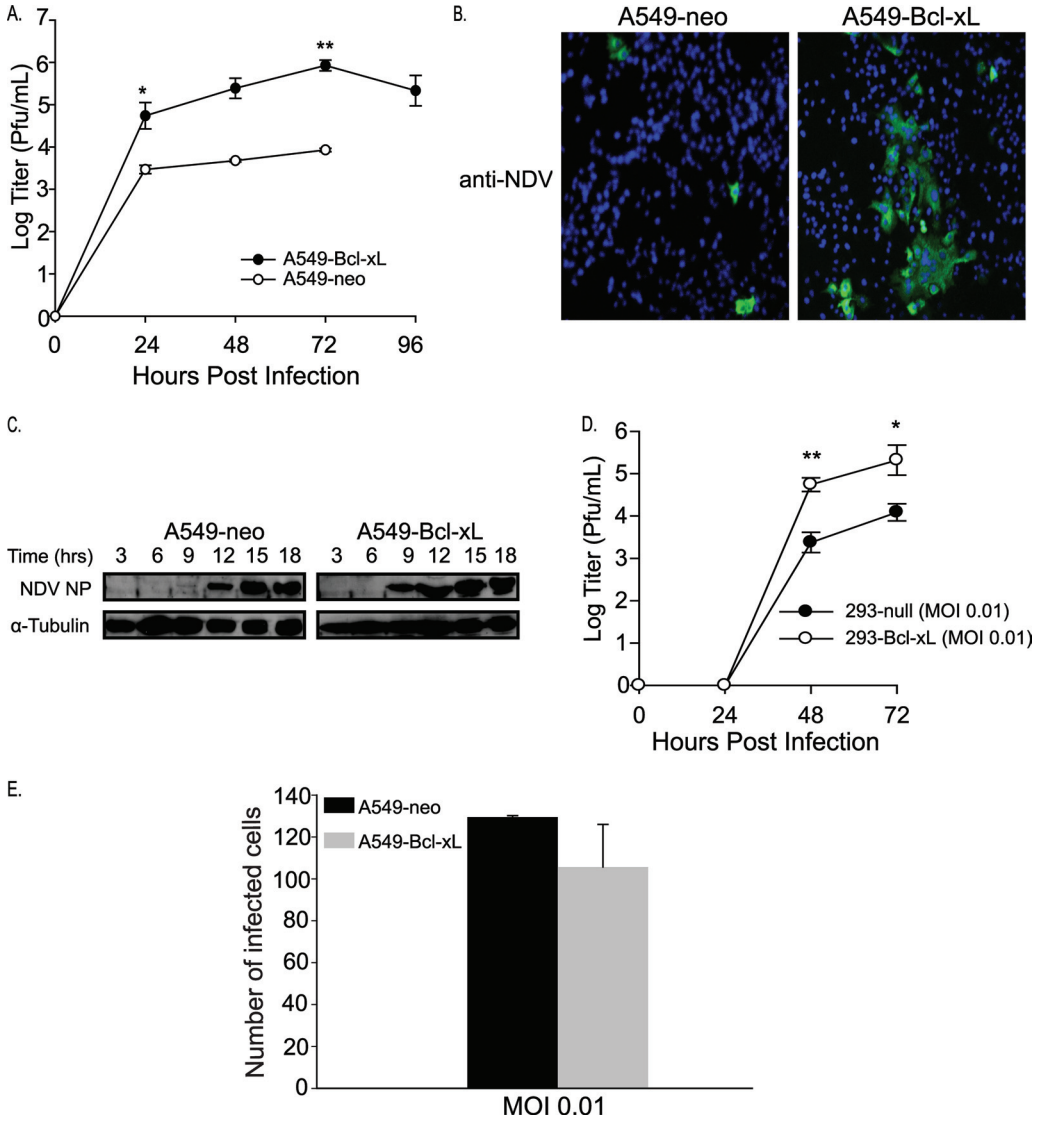

FIG. 5. Enhanced replication of NDV in A549–Bcl-xL cells is associated with enhanced syncytium formation. (A) A549-neo and A549–Bcl-xL cells were infected with NDV(LS)-GFP at an MOI of 0.01, and titers in the supernatants were measured at 24, 48, 72, and 96 h. Note that the 96-h time point value for A549-neo cells was below the detection level. *, $P < 0.04$; **, $P < 0.002$. (B) A549-neo and A549–Bcl-xL cells were infected with NDV (LS)-GFP at an MOI of 0.01, fixed, stained for NDV (green), and assessed for syncytium formation by confocal microscopy. Nuclei were stained with DAPI (blue). (C) Time course of NDV NP expression in A549-neo and A549–Bcl-xL cells. Cells were infected at an MOI of 2 and immunoblotted against anti-tubulin and NDV NP. (D) 293-null and 293-xL cells were infected with NDV (LS)-GFP at an MOI of 0.01, and titers were assessed at 24, 48, and 72 h. *, $P < 0.05$; **, $P < 0.02$. (E) A549-neo and A549–Bcl-xL cells were infected at an MOI of 0.01. Eighteen hours later, cells were fixed and incubated with anti-NDV antibody. Infected cells were counted under a fluorescence microscope. $P = 0.49$.

fixed and counted using immunofluorescence. No significant difference in the number of infected cells between the cell lines was found, indicating that enhanced permissibility to NDV does not play a role in the enhanced oncolytic activity seen in A549–Bcl-xL cells (Fig. 5E). Again, these findings were similar to those we obtained with NDV-NS1 (Fig. 1) (49). As tumor-selective replication of NDV has been associated with defects in the antiviral response (13), we proceeded to determine whether induction of type I IFN played a role in the enhanced oncolytic activity seen in A549–Bcl-xL cells.

NDV activates a type I IFN response in A549–Bcl-xL cells. NDV replication has been linked to defects in the antiviral response of cancer cells. However, in our previous studies and other recent studies, many cancer cell lines have been shown to have a functional and intact IFN response after NDV infection (20, 28, 45, 49). To detect IFN induction in A549-neo and A549–Bcl-xL cells and to demonstrate that the IFN produced inhibits NDV replication, we performed the IFN induction bioassay (Fig. 6A) as previously described (25, 29). Results shown indicate that A549–Bcl-xL cells produce IFN in response to NDV infection that inhibits NDV replication (Fig. 6B). Interestingly, when relative hIFN-β mRNA levels in A549-neo and A549–Bcl-xL cells were compared after NDV infection (Fig. 6C), the amount of IFN-β induced in A549–Bcl-xL cells was significantly higher than that in A549-neo cells, likely secondary to enhanced viral replication. To confirm

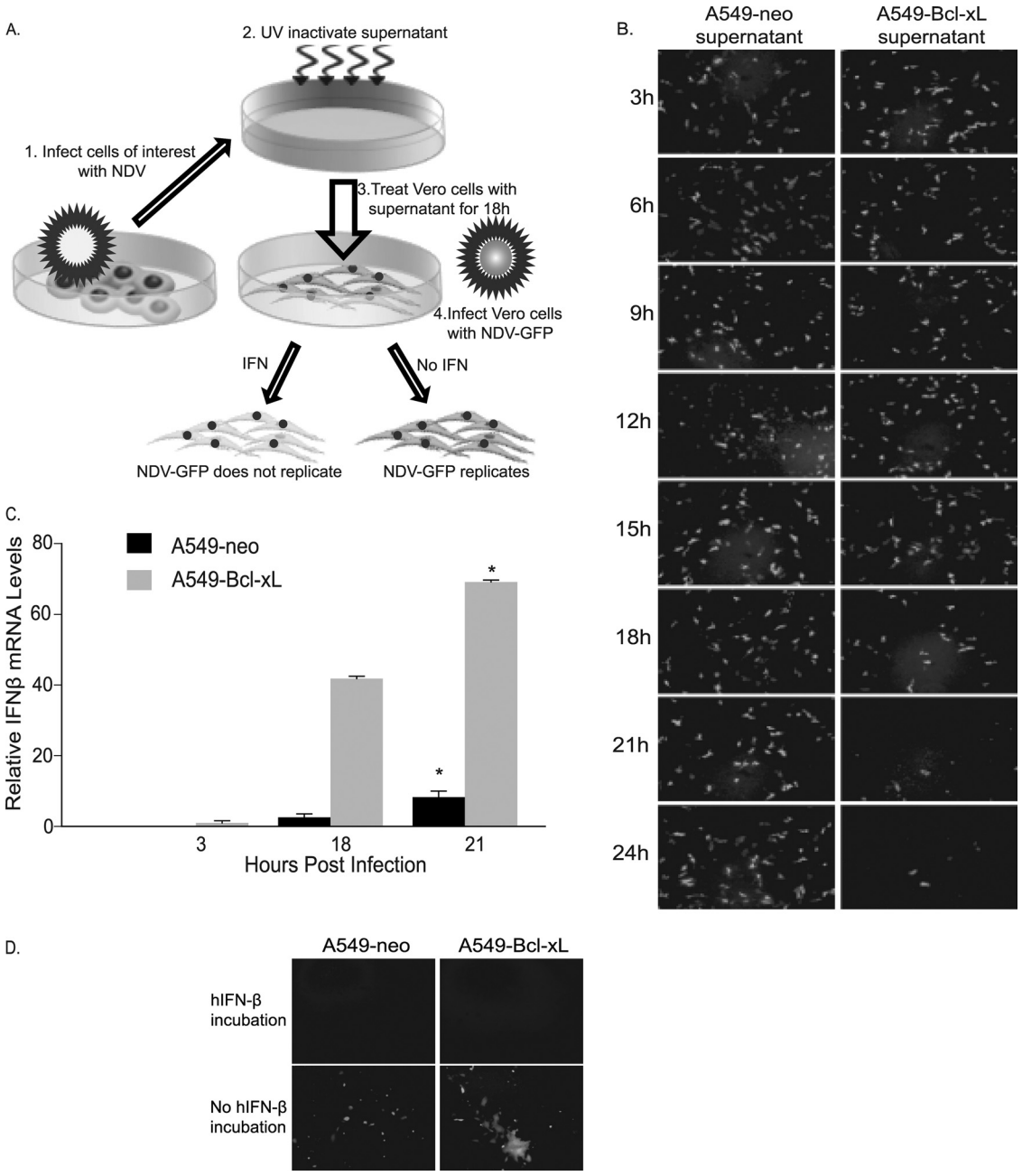

FIG. 6. NDV activates the type I IFN response in both A549-neo and A549–Bcl-xL cells. (A) Schematic diagram of the bioassay for IFN production. Briefly, A549-neo and A549–Bcl-xL cells were infected with NDV at an MOI of 0.1, supernatants were collected at appropriate time points, and then any virus present was UV inactivated. Fresh Vero cells were treated with the inactivated supernatants and then infected with NDV (B1)-GFP at an MOI of 1. (B) Antiviral activity in A549-neo and A549–Bcl-xL cells after NDV infection. Supernatants were collected every 3 h after infection and used in IFN bioassays. (C) hIFN-β mRNA levels in NDV-infected A549-neo and A549–Bcl-xL cells relative to those in noninfected cells measured by qRT-PCR at 3, 18. and 21 hpi. *, $P < 0.03$. (D) A549-neo and A549–Bcl-xL cells were incubated with medium containing 1,000 U of hIFN-β. After 18 h of incubation, cells were washed and infected with NDV (LS)-GFP at an MOI of 0.01 and the GFP signal was assessed at 48 h.

that both cell lines respond to induced IFN, we incubated A549-neo and A549–Bcl-xL cells with medium containing 1,000 U of hIFN-β. After 18 h of incubation, cells were washed and infected with NDV (LS)-GFP at an MOI of 0.01. Pretreatment of cells with hIFN-β inhibited NDV replication, suggesting that the IFN signaling pathway is intact in both A549-neo and A549–Bcl-xL cells (Fig. 6D). Thus, the enhanced oncolytic activity observed in A549–Bcl-xL cells was not secondary to inhibition of type I IFN. On the contrary, enhancement of the type I IFN response was observed in those cells, likely secondary to viral replication to higher titers.

Bcl-xL knockdown inhibits viral replication and syncytium formation in A549–Bcl-xL cells. Our results show that en-

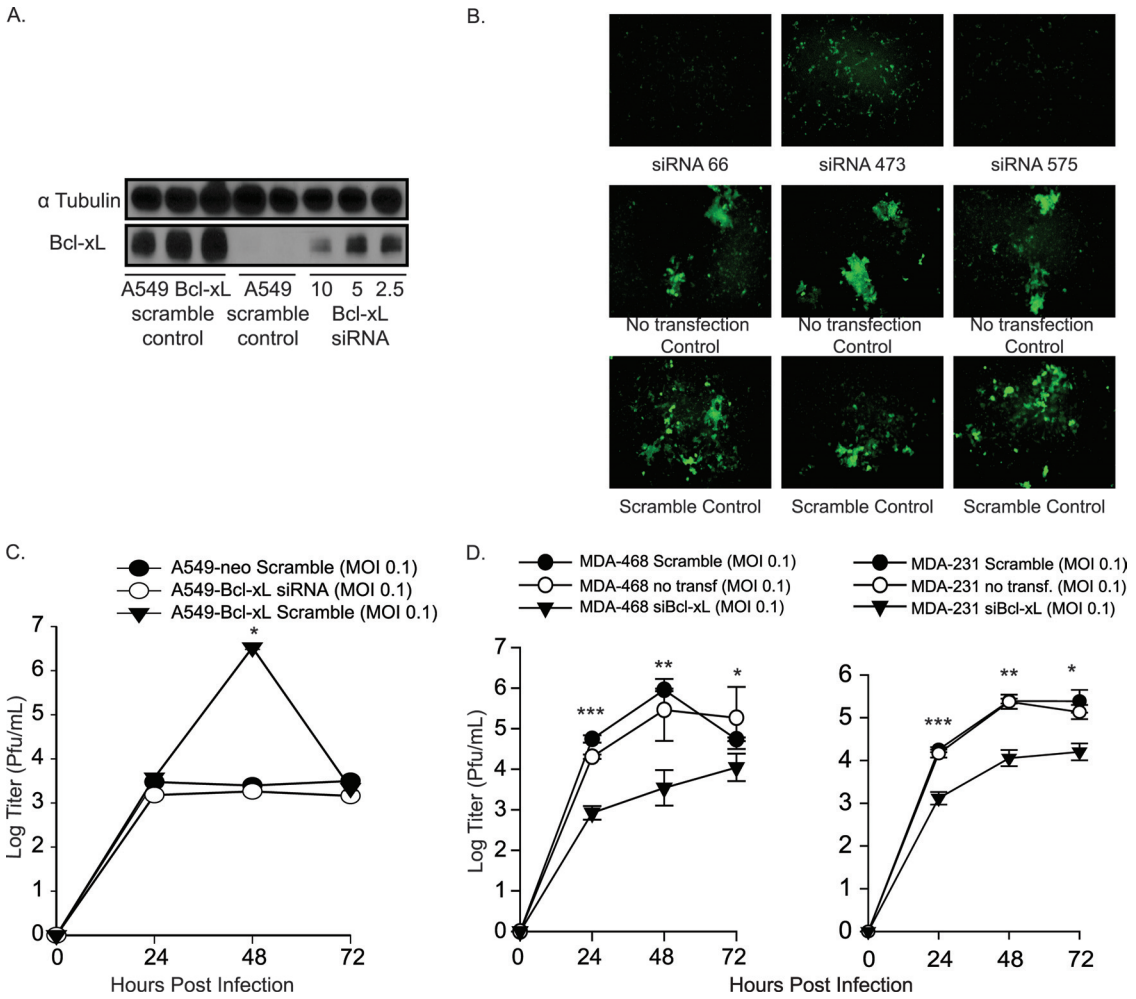

FIG. 7. siRNA knockdown of Bcl-xL in NDV-infected cells reduces oncolytic activity. (A) Western blotting of Bcl-xL knockdown using different amounts of siRNA. (B) A549–Bcl-xL cells were transfected with 5 nM Bcl-xL siRNA or scrambled siRNA and then infected with NDV (LS)-GFP 24 h later. Images were acquired by fluorescence microscopy to assess syncytium formation. (C) Bcl-xL siRNA 575-transfected cells were infected with NDV at an MOI of 0.1, and titers were assessed at 24, 48, and 72 h. *, $P < 0.01$. (D) MDA-MB-231 and MDA-MB-468 cells were transfected with 5 nM Bcl-xL siRNA and infected with NDV (LS)-GFP at an MOI of 0.1. Titers were assessed at the indicated time points. MDA-MB-231: *, $P < 0.004$; **, $P < 0.002$; ***, $P < 7 \times 10^{-6}$. MDA-MB-468: *, $P < 0.02$; **, $P < 0.001$; ***, $P < 0.0009$.

hanced oncolytic activity of NDV in A549–Bcl-xL is due to the antiapoptotic activity of Bcl-xL. To demonstrate that the observed results were due solely to Bcl-xL overexpression and not to another genetic modification of A549–Bcl-xL cells, we knocked down Bcl-xL and analyzed viral replication and syncytium formation. Bcl-xL was knocked down using siRNAs targeting different regions of the Bcl-xL mRNA. Three different siRNAs were tested and demonstrated equivalent inhibitory effects, with representative siRNA 575 shown in Fig. 7A. Syncytium levels were significantly reduced at 48 hpi in A549–Bcl-xL cells after Bcl-xL knockdown relative to those in scrambled-siRNA-transfected and nontransfected controls (Fig. 7B). As expected, this decrease in syncytium formation was accompanied by a decrease in the NDV titer in A549–Bcl-xL cells transfected with scrambled siRNA. NDV-infected A549–Bcl-xL cells transfected with Bcl-xL siRNA showed titers similar to those of A549-neo cells transfected with scrambled siRNA, approximately 1,000-fold lower than the peak NDV titer (Fig. 7C). Overall, these findings suggest that overexpression of Bcl-xL was responsible for enhanced NDV replication and oncolytic activity of NDV and that knockdown of Bcl-xL returns the replication to lower levels. Similar results were observed when endogenous Bcl-xL was knocked down in apoptosis-resistant and chemoresistant breast cancer cell lines MDA-MB-231 and MDA-MB 468 (Fig. 7D) (4). Of note, both cell lines produced IFN in response to viral infection, as determined by IFN bioassay (data not shown).

DISCUSSION

The selectivity of NDV for cancer cells was previously suggested to be due to defects in their antiviral response. However, several studies have shown effective oncolytic activity in cancer cell lines possessing a robust IFN response (20, 28, 39, 40, 49). The ability of NDV to infect IFN-competent cells

suggested that another factor may be responsible for this selectivity.

In our previous study, engineered NDV (F3aa)-NS1 showed enhanced oncolytic activity, which was suggested to be due to IFN antagonism activity of NS1. The antagonism of the innate immune response enhanced NDV replication, in turn making it a more efficient oncolytic agent. In addition, NDV (F3aa)-NS1 demonstrated significant syncytium formation compared to that of NDV (F3aa) not expressing NS1. We proposed that this enhanced syncytium formation was due to the antiapoptotic properties of NS1 brought about by IFN antagonism (49). Enhanced fusogenicity has been shown to improve the oncolytic activity of NDV and vesicular stomatitis virus (1, 7, 35, 40). In NDV-infected cells, syncytia are formed by the accumulation of newly synthesized viral F glycoprotein causing fusion with neighboring cells (17). We postulated that apoptosis resistance may delay the apoptotic death of NDV-infected cells, allowing fusion with an increased number of neighboring cells and thus enhanced syncytium formation. The aim of the present study was to determine the role that cellular resistance to apoptosis may play in the oncolytic activity of NDV.

Bcl-xL is an antiapoptotic protein that in some cancers has been shown to confer resistance to antineoplastic agents (6, 22, 23, 43). By utilizing A549–Bcl-xL cells (Fig. 2), we showed that NDV-mediated cytolysis and fusogenicity are enhanced compared to those in A549-neo cells (Fig. 3 and 5). We confirmed this observation by utilizing a different method of apoptosis inhibition with the use of pan-caspase inhibitor Z-VAD-FMK (Fig. 3). Viral proteins were detected earlier in the infected cells, and viral titers in A549–Bcl-xL cells were significantly higher than in A549-neo cells (Fig. 5), suggesting that enhanced viral replication in the apoptosis-resistant cells was responsible for these findings.

The oncolytic activity in A549–Bcl-xL cells infected with NDV (LS)-GFP was still mediated through apoptosis, though apoptosis was delayed compared to that of infected A549-neo cells (Fig. 4A). We propose that the late apoptosis activation may be due to a combination of overwhelming virus infection during the later cycles, generating cellular stress and activating receptor-mediated apoptosis pathways (8, 31), the RIG-I-activated apoptosis pathway (2), and the proapoptotic activity of IFN (3). In support of the latter, NDV replication in A549–Bcl-xL cells induced a strong type I IFN response (Fig. 6). We suspect that due to Bcl-xL overexpression, activation of apoptosis by antiviral signaling is deficient in A549–Bcl-xL cells, allowing continuous viral replication and type I IFN production, which would explain the elevated levels of type I IFN produced in those cells. This enhancement of early viral replication, in turn, likely translated into a higher number of cells being infected during the subsequent viral replication cycles, which would explain the marked increase in caspase 3 activity and the number of apoptotic cells demonstrated in Fig. 4. This may also provide an explanation for the observed therapeutic activity of the virus in actual tumors, where even a small initial viral inoculum may generate a significant number of viral particles, allowing deeper tumor penetration and oncolysis.

Apoptosis is part of the cellular innate antiviral response (10, 11), and its early activation in infected cells allows rapid elimination of the cell prior to the production of infectious viral progeny. Many viruses have evolved different strategies to inhibit or delay apoptosis induction in order to allow completion of the viral replication cycle and the production of new viruses (15, 33). NDV is no exception; its V protein exhibits antiapoptotic activity in avian cells by blocking IFN (24, 25). To explain the observed oncolytic specificity of NDV, we propose it to be secondary to enhanced replication of NDV in cancer cells, many of which have known defects in apoptotic pathways or overexpress antiapoptotic proteins. After initial virus entry, noncancerous cells quickly undergo apoptosis, resulting in nonproductive infection, while apoptosis-resistant cancer cells survive longer, producing more virus particles and initiating new rounds of infection.

The ability of NDV to induce type I IFN may be an additional benefit for its oncolytic activity. Type I IFN has many tumor suppressor effects that are not fully understood (37), some of which are mediated through the enhancement of apoptosis induction in cancer cells (5) and cell cycle arrest (30). Anticancer properties are mediated either by many IFN-stimulated genes (ISG) or through host-dependent mechanisms that include upregulated expression of major histocompatibility complex class I and II molecules, antigen presentation, memory T cell survival, and $CD8^+$ T cell recruitment (3, 37). Many of these mechanisms have been shown to occur during NDV infection (40, 42, 49, 50).

Our results suggest that NDV may prove to be an attractive oncolytic agent for cancers resistant to multiple chemotherapeutic agents. As mentioned above, many chemoresistant tumors have been associated with apoptosis resistance (6, 22, 23, 43). A recent study demonstrated NDV-HUJ-induced oncolysis in chemoresistant malignant melanoma specimens (20), where chemoresistance has been associated with the IAP Livin (41). NDV may be utilized in the treatment of such tumors either by itself or to sensitize them to chemotherapeutic agents. By activating apoptosis pathways, NDV would also increase the tumor cells' susceptibility to conventional treatment, as a synergistic relationship between oncolytic viruses and chemotherapeutic agents has been described for many viruses (18). In addition, our findings will be useful in the future design of oncolytic NDV vectors, especially ones expressing proteins with antiapoptotic activity. This will move us a step forward in the development of an oncolytic viral vector that is effective against resistant tumors.

ACKNOWLEDGMENTS

We thank Michael A. Pazos for his work on FACS analysis data.

This work was partially supported by Northeast Biodefense grant U54 AI057158 (P.P.) and Bill and Melinda Gates Foundation grant 38648 (P.P.).

The Mount Sinai School of Medicine owns patent positions for reverse genetics of NDVs.

REFERENCES

1. **Altomonte, J., S. Marozin, R. M. Schmid, and O. Ebert.** 2010. Engineered Newcastle disease virus as an improved oncolytic agent against hepatocellular carcinoma. Mol. Ther. **18:**275–284.
2. **Besch, R., et al.** 2009. Proapoptotic signaling induced by RIG-I and MDA-5 results in type I interferon-independent apoptosis in human melanoma cells. J. Clin. Invest. **119:**2399–2411.
3. **Borden, E. C., et al.** 2007. Interferons at age 50: past, current and future impact on biomedicine. Nat. Rev. Drug Discov. **6:**975–990.
4. **Chau, B. N., C. W. Pan, and J. Y. Wang.** 2006. Separation of anti-proliferation and anti-apoptotic functions of retinoblastoma protein through targeted mutations of its A/B domain. PLoS One **1:**e82.
5. **Chawla-Sarkar, M., D. W. Leaman, and E. C. Borden.** 2001. Preferential

induction of apoptosis by interferon (IFN)-beta compared with IFN-alpha2: correlation with TRAIL/Apo2L induction in melanoma cell lines. Clin. Cancer Res. **7:**1821–1831.
6. **Datta, R., et al.** 1995. Overexpression of Bcl-XL by cytotoxic drug exposure confers resistance to ionizing radiation-induced internucleosomal DNA fragmentation. Cell Growth Differ. **6:**363–370.
7. **Ebert, O., et al.** 2004. Syncytia induction enhances the oncolytic potential of vesicular stomatitis virus in virotherapy for cancer. Cancer Res. **64:**3265–3270.
8. **Elankumaran, S., D. Rockemann, and S. K. Samal.** 2006. Newcastle disease virus exerts oncolysis by both intrinsic and extrinsic caspase-dependent pathways of cell death. J. Virol. **80:**7522–7534.
9. **Elmore, S.** 2007. Apoptosis: a review of programmed cell death. Toxicol. Pathol. **35:**495–516.
10. **Everett, H., and G. McFadden.** 1999. Apoptosis: an innate immune response to virus infection. Trends Microbiol. **7:**160–165.
11. **Everett, H., and G. McFadden.** 2001. Viruses and apoptosis: meddling with mitochondria. Virology **288:**1–7.
12. **Fernandez-Sesma, A., et al.** 2006. Influenza virus evades innate and adaptive immunity via the NS1 protein. J. Virol. **80:**6295–6304.
13. **Fiola, C., et al.** 2006. Tumor selective replication of Newcastle disease virus: association with defects of tumor cells in antiviral defence. Int. J. Cancer **119:**328–338.
14. **Freeman, A. I., et al.** 2006. Phase I/II trial of intravenous NDV-HUJ oncolytic virus in recurrent glioblastoma multiforme. Mol. Ther. **13:**221–228.
15. **Hay, S., and G. Kannourakis.** 2002. A time to kill: viral manipulation of the cell death program. J. Gen. Virol. **83:**1547–1564.
16. **Hotte, S. J., et al.** 2007. An optimized clinical regimen for the oncolytic virus PV701. Clin. Cancer Res. **13:**977–985.
17. **Ito, Y., et al.** 1992. Fusion regulation proteins on the cell surface: isolation and characterization of monoclonal antibodies which enhance giant polykaryocyte formation in Newcastle disease virus-infected cell lines of human origin. J. Virol. **66:**5999–6007.
18. **Kumar, S., L. Gao, B. Yeagy, and T. Reid.** 2008. Virus combinations and chemotherapy for the treatment of human cancers. Curr. Opin. Mol. Ther. **10:**371–379.
19. **Lam, K. M., A. C. Vasconcelos, and A. A. Bickford.** 1995. Apoptosis as a cause of death in chicken embryos inoculated with Newcastle disease virus. Microb. Pathog. **19:**169–174.
20. **Lazar, I., et al.** 2010. The oncolytic activity of Newcastle disease virus NDV-HUJ on chemoresistant primary melanoma cells is dependent on the pro-apoptotic activity of the inhibitor of apoptosis protein Livin. J. Virol. **84:**639–646.
21. **Lorence, R. M., et al.** 2007. Phase 1 clinical experience using intravenous administration of PV701, an oncolytic Newcastle disease virus. Curr. Cancer Drug Targets **7:**157–167.
22. **Minn, A. J., C. M. Rudin, L. H. Boise, and C. B. Thompson.** 1995. Expression of bcl-xL can confer a multidrug resistance phenotype. Blood **86:**1903–1910.
23. **Nuessler, V., et al.** 1999. Bcl-2, bax and bcl-xL expression in human sensitive and resistant leukemia cell lines. Leukemia **13:**1864–1872.
24. **Park, M. S., A. Garcia-Sastre, J. F. Cros, C. F. Basler, and P. Palese.** 2003. Newcastle disease virus V protein is a determinant of host range restriction. J. Virol. **77:**9522–9532.
25. **Park, M. S., et al.** 2003. Newcastle disease virus (NDV)-based assay demonstrates interferon-antagonist activity for the NDV V protein and the Nipah virus V, W, and C proteins. J. Virol. **77:**1501–1511.
26. **Pfaffl, M. W.** 2001. A new mathematical model for relative quantification in real-time RT-PCR. Nucleic Acids Res. **29:**e45.
27. **Prince, A. M., and H. S. Ginsberg.** 1957. Studies on the cytotoxic effect of Newcastle disease virus (NDV) on Ehrlich ascites tumor cells. I. Characteristics of the virus-cell interaction. J. Immunol. **79:**94–106.
28. **Puhlmann, J., F. Puehler, D. Mumberg, P. Boukamp, and R. Beier.** 2010. Rac1 is required for oncolytic NDV replication in human cancer cells and establishes a link between tumorigenesis and sensitivity to oncolytic virus. Oncogene **29:**2205–2216.
29. **Quinlivan, M., et al.** 2005. Attenuation of equine influenza viruses through truncations of the NS1 protein. J. Virol. **79:**8431–8439.
30. **Randall, R. E., and S. Goodbourn.** 2008. Interferons and viruses: an interplay between induction, signalling, antiviral responses and virus countermeasures. J. Gen. Virol. **89:**1–47.
31. **Ravindra, P. V., et al.** 2009. Time course of Newcastle disease virus-induced apoptotic pathways. Virus Res. **144:**350–354.
32. **Reichard, K. W., et al.** 1992. Newcastle disease virus selectively kills human tumor cells. J. Surg. Res. **52:**448–453.
33. **Roulston, A., R. C. Marcellus, and P. E. Branton.** 1999. Viruses and apoptosis. Annu. Rev. Microbiol. **53:**577–628.
34. **Schulze, T., et al.** 2009. Efficiency of adjuvant active specific immunization with Newcastle disease virus modified tumor cells in colorectal cancer patients following resection of liver metastases: results of a prospective randomized trial. Cancer Immunol. Immunother. **58:**61–69.
35. **Shin, E. J., et al.** 2007. Fusogenic vesicular stomatitis virus for the treatment of head and neck squamous carcinomas. Otolaryngol. Head Neck Surg. **136:**811–817.
36. **Sinkovics, J. G., and J. C. Horvath.** 2000. Newcastle disease virus (NDV): brief history of its oncolytic strains. J. Clin. Virol. **16:**1–15.
37. **Smyth, M. J.** 2005. Type I interferon and cancer immunoediting. Nat. Immunol. **6:**646–648.
38. **Stojdl, D. F., et al.** 2000. Exploiting tumor-specific defects in the interferon pathway with a previously unknown oncolytic virus. Nat. Med. **6:**821–825.
39. **Vigil, A., O. Martinez, M. A. Chua, and A. Garcia-Sastre.** 2008. Recombinant Newcastle disease virus as a vaccine vector for cancer therapy. Mol. Ther. **16:**1883–1890.
40. **Vigil, A., et al.** 2007. Use of reverse genetics to enhance the oncolytic properties of Newcastle disease virus. Cancer Res. **67:**8285–8292.
41. **Vucic, D., H. R. Stennicke, M. T. Pisabarro, G. S. Salvesen, and V. M. Dixit.** 2000. ML-IAP, a novel inhibitor of apoptosis that is preferentially expressed in human melanomas. Curr. Biol. **10:**1359–1366.
42. **Washburn, B., and V. Schirrmacher.** 2002. Human tumor cell infection by Newcastle disease virus leads to upregulation of HLA and cell adhesion molecules and to induction of interferons, chemokines and finally apoptosis. Int. J. Oncol. **21:**85–93.
43. **Watanabe, J., et al.** 2004. Prognostic significance of Bcl-xL in human hepatocellular carcinoma. Surgery **135:**604–612.
44. **Wong, J., et al.** 2010. Detection of free peritoneal cancer cells in gastric cancer using cancer-specific Newcastle disease virus. J. Gastrointest. Surg. **14:**7–14.
45. **Yaacov, B., et al.** 2008. Selective oncolytic effect of an attenuated Newcastle disease virus (NDV-HUJ) in lung tumors. Cancer Gene Ther. **15:**795–807.
46. **Youle, R. J., and A. Strasser.** 2008. The BCL-2 protein family: opposing activities that mediate cell death. Nat. Rev. Mol. Cell Biol. **9:**47–59.
47. **Yuan, B., R. Latek, M. Hossbach, T. Tuschl, and F. Lewitter.** 2004. siRNA Selection Server: an automated siRNA oligonucleotide prediction server. Nucleic Acids Res. **32:**W130–W134.
48. **Zamarin, D., A. Garcia-Sastre, X. Xiao, R. Wang, and P. Palese.** 2005. Influenza virus PB1-F2 protein induces cell death through mitochondrial ANT3 and VDAC1. PLoS Pathog. **1:**e4.
49. **Zamarin, D., et al.** 2009. Enhancement of oncolytic properties of recombinant Newcastle disease virus through antagonism of cellular innate immune responses. Mol. Ther. **17:**697–706.
50. **Zamarin, D., A. Vigil, K. Kelly, A. Garcia-Sastre, and Y. Fong.** 2009. Genetically engineered Newcastle disease virus for malignant melanoma therapy. Gene Ther. **16:**796–804.
51. **Zhirnov, O. P., T. E. Konakova, T. Wolff, and H. D. Klenk.** 2002. NS1 protein of influenza A virus down-regulates apoptosis. J. Virol. **76:**1617–1625.